Topological Polaritons

Torsten Karzig,[1] Charles-Edouard Bardyn,[1] Netanel H. Lindner,[2,1] and Gil Refael[1]
[1]*Institute for Quantum Information and Matter, Caltech, Pasadena, California 91125, USA*
[2]*Physics Department, Technion, 320003 Haifa, Israel*
(Received 25 August 2014; revised manuscript received 29 January 2015; published 1 July 2015)

The interaction between light and matter can give rise to novel topological states. This principle was recently exemplified in Floquet topological insulators, where *classical* light was used to induce a topological electronic band structure. Here, in contrast, we show that mixing *single* photons with excitons can result in new topological polaritonic states—or "topolaritons." Taken separately, the underlying photons and excitons are topologically trivial. Combined appropriately, however, they give rise to nontrivial polaritonic bands with chiral edge modes allowing for unidirectional polariton propagation. The main ingredient in our construction is an exciton-photon coupling with a phase that winds in momentum space. We demonstrate how this winding emerges from the finite-momentum mixing between s-type and p-type bands in the electronic system and an applied Zeeman field. We discuss the requirements for obtaining a sizable topological gap in the polariton spectrum and propose practical ways to realize topolaritons in semiconductor quantum wells and monolayer transition metal dichalcogenides.

DOI: 10.1103/PhysRevX.5.031001

Subject Areas: Condensed Matter Physics, Optoelectronics, Photonics

I. INTRODUCTION

The idea of creating topological photonic states was established in 2008 [1,2]. In a seminal work, Haldane and Raghu proposed to generate the analog of quantum-Hall states in photonic crystals with broken time-reversal symmetry. Shortly thereafter, this concept was experimentally demonstrated for electromagnetic waves in the microwave domain [3,4]. Topological photonic states at optical frequencies, however, suffer from the fact that the magnetic permeability is essentially $\mu = 1$ in this regime [5], which renders the magneto-optical response that allows to break time-reversal symmetry very weak. Proposed alternatives include the use of time-periodic systems [6,7], coupled optical resonators or cavities [8–14], as well as metamaterials [15–17]. Despite the accompanying experimental progress [3,4,7,12], the realization of photonic states with true topological protection at optical frequencies remains challenging.

Here, we pursue a new direction motivated by the concept of Floquet topological insulators [18], which rely on the specific mixing of two topologically trivial fermionic bands made possible by the absorption or emission of photons. In contrast to using photons to generate a nontrivial topology, we ask whether one can reverse this concept and create a nontrivial photon topology with the help of electronic degrees of freedom. We show that this is indeed possible by coupling photons to semiconductor excitons. Although both of these ingredients are ordinary (nontopological) by themselves, their combination can lead to new (quantum-Hall-like) topological states of polaritons which we call, in short, "topolaritons." We consider a setup where band mixing between s and p bands couples photons and excitons in a nontrivial way. In combination with time-reversal symmetry breaking for the underlying semiconductor (e.g., by a Zeeman field), we demonstrate that it is possible to generate a nontrivial topology.

In contrast to quantum-Hall states of fermions, the topology of the bosonic (polariton) system that we consider is not a ground-state property. Instead, it is characterized by topological bands in the excitation spectrum. The main

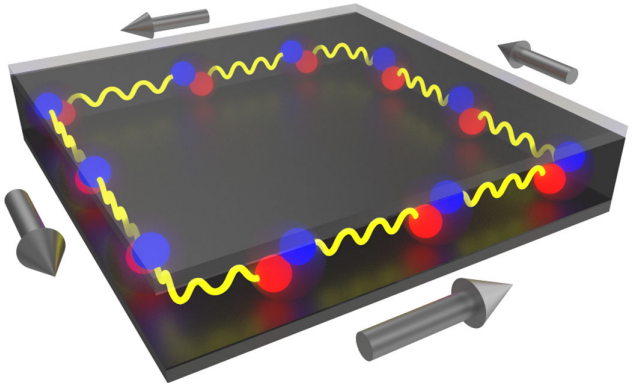

FIG. 1. Schematic view of a system with topological polaritons. A chiral polaritonic mode consisting of a mixture of bound particle-hole pairs (excitons) and photons is found at the edge of the system.

signature of this nontrivial topology is a bulk gap in the excitation spectrum with chiral edge modes as the only in-gap states (see Fig. 1). These edge modes provide a new realization of a controllable one-way waveguide for photons [3,4,19–23]. More conceptually, our proposal allows to realize topological photons at optical frequencies and, to the best of our knowledge, constitutes the first example of a topological hybrid state treating light and matter degrees of freedom on the same footing. This is particularly interesting since finite interactions in the excitonic component open the perspective of interacting topological states of polaritons.

II. TOPOLARITONS

Polaritons are superpositions of photons and excitons that can be described by a Hamiltonian of the form

$$\hat{H} = \sum_{\mathbf{q}} [\omega_q^C \hat{a}_{\mathbf{q}}^\dagger \hat{a}_{\mathbf{q}} + \omega_q^X \hat{b}_{\mathbf{q}}^\dagger \hat{b}_{\mathbf{q}} + (g_{\mathbf{q}} \hat{b}_{\mathbf{q}}^\dagger \hat{a}_{\mathbf{q}} + \text{H.c.})], \quad (1)$$

where the operators $\hat{a}_{\mathbf{q}}^\dagger$ and $\hat{b}_{\mathbf{q}}^\dagger$ create photons and excitons with momentum $\mathbf{q}$, respectively. We assume that the excitons and photons are both confined to two dimensions; i.e., $\mathbf{q} = (q_x, q_y)$. For the excitons, this can be achieved using a quantum well, while photons can be trapped using a microcavity or waveguide. The exciton dispersion $\omega_q^X = q^2/2m_X + \omega_0^X$ (setting $\hbar = 1$) describes its center-of-mass motion, while the energy gap ω_0^X for creating an exciton is given by the difference between the bare particle-hole excitation gap and the exciton binding energy. We denote the dispersion of the cavity photon by ω_q^C.

The crucial ingredient for generating topolaritons is the exciton-photon coupling $g_{\mathbf{q}}$, which describes the creation of an exciton by photon absorption and vice versa. Here, we require $g_{\mathbf{q}}$ to wind according to

$$g_{\mathbf{q}} = g_q e^{im\theta_{\mathbf{q}}}, \quad (2)$$

where g_q is the amplitude of the exciton-photon interaction (or Rabi frequency), m is a nonzero integer, and $\theta_{\mathbf{q}}$ denotes the polar angle of $\mathbf{q}$.

To reveal the nontrivial topology, we diagonalize the Hamiltonian Eq. (1) in terms of polariton operators

$$\hat{P}_{\mathbf{q}}^{\pm} = \mathbf{e}_{\mathbf{q}}^{P\pm} \cdot \begin{pmatrix} \hat{a}_{\mathbf{q}} \\ \hat{b}_{\mathbf{q}} \end{pmatrix}, \quad (3)$$

with spectrum $\omega_q^{P\pm} = \frac{1}{2}(\omega_q^C + \omega_q^X) \pm \frac{1}{2}[(\omega_q^C - \omega_q^X)^2 + 4g_q^2]^{1/2}$, where the $\pm$ sign refers to the upper and lower polariton band, respectively (see Fig. 2). The vectors $\mathbf{e}_{\mathbf{q}}^{P\pm}$ describe the relative strength between the photon and exciton components of the polariton wave function and can be interpreted as a spinor. The nontrivial form of the coupling Eq. (2) leads to a winding of this spinor of the form

$$\mathbf{e}_{\mathbf{q}}^{P\pm} = \frac{1}{\sqrt{2}} \begin{pmatrix} \pm e^{-im\theta_{\mathbf{q}}} \sqrt{1 \pm \beta_q} \\ \sqrt{1 \mp \beta_q} \end{pmatrix} \quad (4)$$

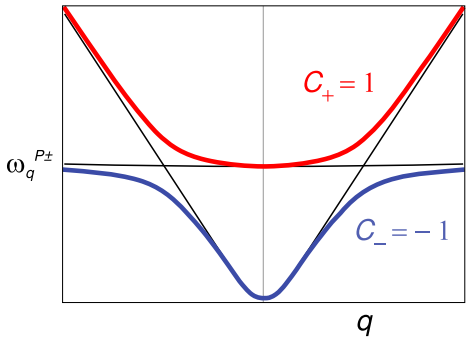

FIG. 2. Schematic polariton spectrum $\omega_q^{P\pm}$. The upper and lower polariton bands are drawn in red and blue, while the uncoupled bands ($g_q = 0$) are shown as thin black lines for comparison. Because of the winding structure of the coupling, the two polariton bands acquire a nontrivial topology with finite Chern numbers $C_\pm = \pm 1$ in the case of $m = 1$ [see Eq. (2)]. The associated edge modes are indicated by a dashed purple line.

where $\beta_q = (\omega_q^C - \omega_q^X)/[(\omega_q^C - \omega_q^X)^2 + 4g_q^2]^{1/2}$. The spinor of the lower polariton band "flips" from photonic to excitonic (vice versa for the upper polariton) far away from the resonance as described by the limits $\beta_{q=0} = -1$ and $\beta_{q\to\infty} = 1$. Combined with the winding $e^{im\theta_{\mathbf{q}}}$, this flip leads to a full wrapping of the unit sphere by the spinor $\mathbf{e}_{\mathbf{q}}^{P\pm}$, thereby leading to a nontrivial topology in full analogy to fermionic topological systems. This can be confirmed by calculating the Chern number of the upper and lower polariton bands. Indeed, we find $C_\pm = \pm m$. Note that the mechanism leading to nontrivial topology is distinctly different from the original proposal by Haldane and Raghu [1,2]. Here, the nontrival Berry curvature arises directly from the (winding) hybridization between two ordinary exciton and photon bands, not from the gapping out of symmetry-protected band touchings (e.g., Dirac cones) in the photonic spectrum [24].

A consequence of the nontrivial Chern number is the presence of chiral polaritonic edge modes. In our setting, edges are defined by the confinement of the excitons and photons. While excitons are naturally restricted to the quantum well, photons can be confined, e.g., by using reflecting mirrors or a suitable photonic band gap at the edges of the system. Another possibility would be to confine the photons in a dielectric slab waveguide ending at the system edges.

Besides the existence of bands with nontrivial Chern numbers, the stability of the edge modes also requires a global energy gap (i.e., present for all momenta) between the upper and lower polariton bands. Above, we assume that the bare exciton and photon dispersions are far (negatively) detuned at $q = 0$. In that case, the energy of the lower polariton branch essentially coincides with the bare exciton dispersion for low momenta. Since the lower polariton branch approaches the bare exciton dispersion for large q, it thus appears impossible to open a gap for a

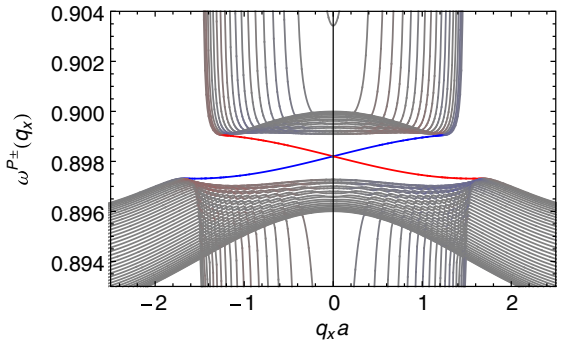

FIG. 3. Topological polariton spectrum. Spectrum obtained for a tight-binding lattice analog of the Hamiltonian Eq. (1) on a square lattice with periodic (open) boundary conditions in the x direction (y direction). Two edge modes are found within the gap, each localized at one of the system boundaries. The color scale encodes the edge localization, where red (blue) indicates a large weight of the wave function at the edge at $y = 0$ ($y = L$). For the construction of the lattice model, we choose quadratic dispersions $q^2/2m_X + \omega_0^X$ and $q^2/2m_C$ for the exciton and photon, respectively, replacing $q_{x,y}^2 \to 2 - 2\cos(q_{x,y})$ (note that a quadratic photon dispersion with $m_C = q_{\mathrm{res}}/2c$ correctly reproduces the original linear dispersion close to resonance at q_{res}). Similarly, we model the winding coupling by $g_{\mathbf{q}} = g[\sin(q_x) + i\sin(q_y)]$. The system size is 40×40 (with lattice constant $a = 1$), and the other relevant parameters are given by $m_X = -500$, $m_C = 1$, $\omega_0^X = 0.25$, and $g = 0.01$.

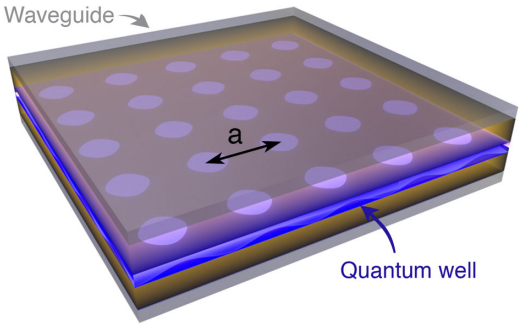

FIG. 4. Schematic experimental setup for realizing topolaritons. A quantum well (in blue) is embedded in a photonic waveguide (or cavity). The boundary of the light blue disks represent equipotential lines of the periodic exciton potential with lattice constant a (see Sec. IIIB).

positive exciton mass. Although a small gap can in principle be opened by considering a negative exciton mass, as depicted in Fig. 3, we present below a more realistic and efficient way to realize topolaritons. We first discuss how to obtain a winding exciton-photon coupling, and show that a sizable topological gap can be opened in the presence of a periodic exciton potential.

III. REALIZING TOPOLARITONS

A. Winding coupling

Promising candidates for the realization of topolaritons are semiconductor quantum wells embedded in photonic waveguides or microcavities (Fig. 4). One of the main requirements is the presence of a single (bright) two-dimensional excitonic mode. Here, we consider the standard case of excitons formed from s-type electronic states in the conduction band and p-type heavy-hole states in the valence band. The essential part of the quantum well $k \cdot p$ Hamiltonian describing these particle and hole bands can be expressed in the form [25]

$$H_{\mathrm{QW}} = \left(M + \frac{k^2}{2m}\right)\sigma_z + A(k_x\sigma_x + k_y\sigma_y), \qquad (5)$$

where $M > 0$ determines the size of the (trivial) band gap, σ_i are Pauli matrices corresponding to states with different total angular momentum ($J_z = -1/2$ and $J_z = -3/2$), and A describes the finite-momentum interband mixing.

The original $k \cdot p$ Hamiltonian also includes the time-reversed version of H_{QW} (involving $J_z = 1/2$ and $J_z = 3/2$ states). Here, we break time-reversal symmetry and isolate a single one of these blocks by applying an external magnetic field in the z direction. A finite Zeeman field can shift the exciton energy when the conduction and valence bands have different g factors. Below, we assume that the resulting energy splitting between excitons belonging to different blocks is large enough so that one can focus on a single one of them. We note that this strict separation is only justified provided that the Zeeman splitting is larger than the exciton-photon coupling. Our results, however, remain valid for much weaker Zeeman fields (only exceeding the size of the topological gap). Taking into account both excitons, we find two topological gaps energetically separated by the Zeeman splitting, with respective edge states of opposite chirality (see Supplemental Material [26]). We remark that orbital effects of the magnetic field can be neglected as long as the magnetic length is larger than the size of the excitons, which we assume in what follows.

When adding Coulomb interactions to the quantum-well Hamiltonian Eq. (5), excitons form as bound states of conduction-band particles and valence-band holes. The Bohr radius a_0 of such "particle-hole atoms" is typically of the order of 1–10 nm, with binding energies of the order of 10–100 meV (see, e.g., Ref. [27]). Expressed in terms of the creation operators $\hat{c}_{c,\mathbf{k}}^\dagger$ and $\hat{c}_{v,\mathbf{k}}$ for conduction-band particles and valence-band holes, the corresponding exciton operator takes the form

$$\hat{b}_{\mathbf{q}}^{(n)\dagger} = \sum_{\mathbf{k}} \phi_n(\mathbf{k})\hat{c}_{c,\mathbf{k}+\mathbf{q}/2}^\dagger \hat{c}_{v,\mathbf{k}-\mathbf{q}/2} \qquad (6)$$

and obeys bosonic commutation relations for low exciton densities (note that we assume equal masses for particles and holes, for simplicity). The exciton wave functions $\phi_n(\mathbf{k})$ are (the Fourier transform of) hydrogen-atom-like

wave functions in relative coordinates for the bound particle-hole pairs.

For the photonic part of the Hamiltonian, we assume that the photons are confined to two dimensions by a waveguide or a microcavity (the semiconductor quantum well being either in direct proximity or inside the latter). The two-dimensional photonic modes are of either TE or TM nature. To open a gap in the polariton spectrum, we want to target a regime where a single photonic mode couples to a single excitonic mode. This can be realized by using a photonic crystal with a suitably tailored TM band gap (see e.g., Ref. [28]) where the presence of TM modes within the topological gap is avoided.

We remark that it is in principle also possible to observe topological features in the absence of a TM gap, in the limit of large in-plane momentum around the exciton-photon resonance $q_{\rm res}$. In this regime, the electric field of the TM mode points predominantly out of the plane. Since two-dimensional excitons couple only to in-plane electric fields, the coupling to the TM modes vanishes in this limit, suppressed by a factor of $1/(q_{\rm res}d)$, where d is the thickness of the waveguide or microcavity. In practice, the (finite but small) coupling of excitons to TM modes will lead to some mixing of the resulting chiral edge states with the TM modes, which spoils true topological protection. For theoretical clarity, we focus on the TE mode in the following, and discuss the details of the TE-TM interplay in the Supplemental Material [26].

The quantized vector potential describing the TE modes takes the form

$$e\hat{\mathbf{A}}(\mathbf{r},t)=\int\frac{dq^2}{(2\pi)^2}F_{\mathbf{q}}(\mathbf{e}_{\mathbf{q}\perp}\hat{a}_{\mathbf{q}}e^{i(\mathbf{q}\cdot\mathbf{r}-\omega_{\mathbf{q}}t)}+\text{H.c.}),\quad(7)$$

where $\hat{a}^\dagger_{\mathbf{q}}$ creates a photon of momentum $\mathbf{q}$, $\mathbf{e}_{\mathbf{q}\perp}=(-q_y,q_x)/q$ describes the direction of the in-plane electric field perpendicular to the propagation direction $\mathbf{q}$, and $F_{\mathbf{q}}=[e^2/(2\epsilon w\omega^C_{\mathbf{q}})]^{1/2}$, where e denotes the electron charge, ϵ the dielectric constant, and w the width of the waveguide or microcavity in the z direction. The coupling of the photons to the quantum well can be incorporated by the standard substitution $\mathbf{k}\to\mathbf{k}+e\hat{\mathbf{A}}$ in the Hamiltonian Eq. (5). The mixing between the s and p bands in the quantum well, combined with the locking of the electric-field direction ($\mathbf{e}_{\mathbf{q}\perp}$) to $\mathbf{q}$, then leads to a winding exciton-photon coupling. For s-wave excitons, and provided that $A/(Ma_0)<1$ (see appendixes), we find an exciton-photon Hamiltonian of the form Eq. (1), with a winding coupling

$$g_{\mathbf{q}}\approx -i\sqrt{\frac{2}{\pi}}\frac{A}{a_0}F_{\mathbf{q}}e^{-im\theta_{\mathbf{q}}},\quad(8)$$

where $m=1$. Intuitively, this single winding can be understood from the fact that angular momentum conservation is required when mixing excitons with total angular momentum projection $J_z=1$ with the (linearly polarized) TE mode of $J_z=0$. Higher winding numbers $m=\pm2$ can in principle be achieved starting from excitons with $J_z=\pm1$ coupled to photons with helicity ∓1. We detail this alternative scheme in the Supplemental Material [26]. As far as higher winding numbers are concerned, it would also be interesting to extend our proposal to systems in which excitons already have a nontrivial topological nature [29–31].

Note that despite its winding form, the coupling of Eq. (8) originates from the same dipole moment as the standard (constant) coupling Ω of $J_z=+1$ (-1) excitons to right- (left-)handed polarized light. This can be seen from the small momentum limit, where the right-handed polarized mode is given by $a^+_{\mathbf{q}}=(a^{\rm TM}_{\mathbf{q}}-ia^{\rm TE}_{\mathbf{q}})e^{-i\theta_{\mathbf{q}}}/\sqrt{2}$ (see Supplemental Material [26]), yielding $|g_{\mathbf{q}}|=\Omega/\sqrt{2}$.

B. Finite topological gap

The remaining ingredient for chiral polaritonic edge modes is a finite topological gap. One way to open such a gap is to introduce a periodic potential in the coupled exciton-photon system (see Fig. 4). While periodic potentials for photons are naturally provided by photonic crystals [32], excitonic analogs can be realized, e.g., by applying strain to the quantum well (see Ref. [33] and references therein) or using surface acoustic waves [34,35]. The presence of a periodic potential with period a introduces a Brillouin zone for the polariton spectrum. The coupling of the backfolded bands at the Brillouin-zone boundary then allows one to open a gap (see Fig. 5).

To understand the topological nature of such a gap, we recall that most of the winding responsible for the nontrivial topology takes place around the circle of radius $q_{\rm res}$ corresponding to the exciton-photon resonance. For $\pi/a>q_{\rm res}$, we thus expect the same nontrivial Chern

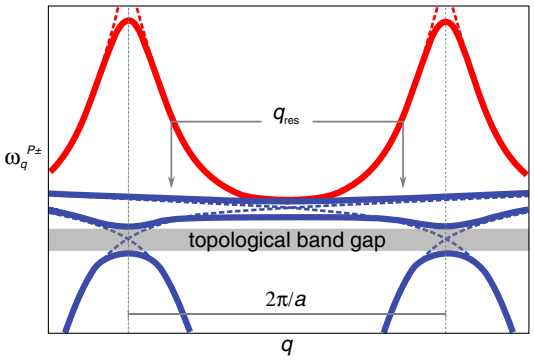

FIG. 5. Scheme for opening a topological gap using a periodic potential. The solid (dashed) blue and red lines correspond to the dispersion of the lower and upper polaritons with (without) a periodic potential in a simplified one-dimensional scenario. As long as $\pi/a>q_{\rm res}$, the lowest polariton band includes the winding around the resonance and the gap opened at the Brillouin-zone boundary is of topological nature.

number as in the absence of a periodic potential, while for $\pi/a < q_{\mathrm{res}}$, the lowest polariton band should be topologically trivial. To achieve a large topological gap, the Brillouin-zone boundary should correspond to a momentum of the order of (but larger than) q_{res}.

Note that opening a topological gap in the exciton-dominated polariton regime (i.e., at $q > q_{\mathrm{res}}$) requires a periodic exciton potential. In particular, it is not possible to use purely photonic periodic potentials. The latter can gap out the excitonic part only via the (winding) exciton-photon coupling $g_{\mathbf{q}}$. This results in an additional winding coupling between the excitonic bands at the Brillouin-zone boundary, which cancels the original winding and makes the gap between the lowest polariton bands topologically trivial. Note that, due to the weaker effect of photonic potentials on the exciton-dominated regime, including periodic exciton and photon potentials will, in general, still lead to topological gaps [36]. To simplify the discussion, here we focus on periodic potentials that are purely excitonic and discuss the case of both exciton and photon potentials in the Supplemental Material [26].

Figure 5 provides an intuitive picture of our gap-opening scheme in a simplified one-dimensional case. For the actual two-dimensional Brillouin zone, one essentially recovers this scenario for any cut passing through the center of the Brillouin zone (see appendixes). The optimal way to open a topological gap is to maximize the overlap between the gaps obtained along each possible cut. This occurs when the Brillouin-zone geometry is as circular as possible (e.g., hexagonal).

C. Numerical results

To study the edge modes numerically, we start from the same lattice model as in Fig. 3 and set the lattice constant to $a/2$. We then introduce a periodic potential of period a by alternating the on-site energy between neighboring sites of the square lattice. Figure 6 shows the resulting spectrum, which clearly demonstrates the presence of polaritonic edge modes. Since the topological gap Δ is controlled by the periodic potential, we find that the typical length scale for the edge-mode localization is of the order of a (see Fig. 6, where the extent of the edge modes in momentum space is of the order of π/a). The size of the gap then determines the edge-mode velocity $v \sim a\Delta/\pi$. Since the exciton velocity is essentially negligible as compared to the photon velocity c, the edge-mode velocity in turn dictates a ratio v/c between the photon and exciton components of the edge mode.

D. Practical realization

What are the necessary features and parameters for a quantum well to host topolaritons? Most importantly, it must support free excitons. In addition, the exciton-photon coupling $g_{\mathbf{q}}$ must be as large as possible since it defines, along with the periodic exciton potential, the relevant gaps in the polariton spectrum. Equation (8) ties $g_{\mathbf{q}}$ to the ratio of

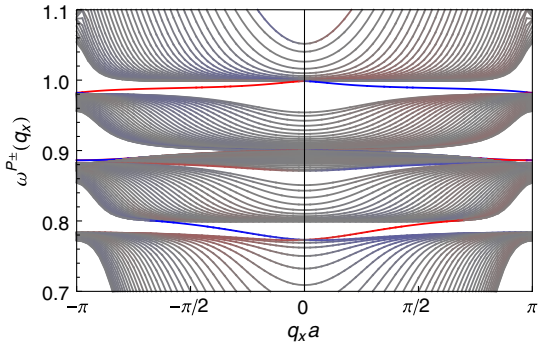

FIG. 6. Topological polariton spectrum with a periodic potential. The spectrum is obtained for a finite-size lattice version of the Hamiltonian Eq. (1) with an additional periodic potential of period a and exhibits in-gap chiral edge modes (colored). The color scale encodes the edge localization, where red (blue) indicates a large weight of the wave function at the edge at $y = 0$ ($y = L$). The system size is 40×40 (with lattice constant $a = 1$) and the other relevant parameters are given by $m_X = 1 \times 10^5$, $m_C = 1$, $\omega_0^X = 0.9$, $g = 0.1$,$V_X = 0.05$.

the finite-momentum interband-mixing amplitude A to the exciton Bohr radius a_0, and is valid provided that $A/a_0 < M$ [see also Eq. (5)]. Together, the above conditions thus require a large dipole moment (controlling A) and a band gap larger than A/a_0. The size of the topological gap is ultimately limited by the strength of the periodic exciton potential and by the exciton Zeeman splitting. A crucial requirement for the resulting gap is that it exceeds the inverse polariton lifetime, such that the topological edge modes are well defined despite the decay-induced broadening of the polariton states.

We demonstrate the feasibility of our proposal using CdTe-based quantum wells as a guideline. For an exciton energy $\omega_0^X = 1.6$ eV and a dielectric constant $\epsilon = 8$, the condition $\pi/a \sim q_{\mathrm{res}}$ is fulfilled for a periodic exciton potential with lattice constant $a \approx 150$ nm. CdTe-based quantum wells are a standard platform to reach the strong-coupling limit. Recently, exciton-photon couplings of up to $\Omega = \sqrt{2}|g_{\mathbf{q}}| = 55$ meV have been reached using multiple CdTe-based quantum wells ($\Omega = 5.4$ meV for a single quantum well) embedded in a photonic-crystal-based microcavity [37]. For such large exciton-photon couplings, the size of the topological gap would essentially be limited by only the strength of the periodic exciton potential and the exciton Zeeman splitting. For more moderate exciton-photon couplings $\Omega = 20$ meV and an optimal triangular-lattice potential of depth 1 meV, a topological gap of 0.3 meV can be obtained. Such a gap would be large enough to achieve stable polariton edge modes, since typical polariton lifetimes are of the order of tens of picoseconds (1/10 ps = 0.07 meV) [27]. With a typical exciton g factor of about 2 [38], the Zeeman energy would not be a limiting factor for the above topological gap of 0.3 meV when applying magnetic fields of 2.5 T or larger.

A promising alternative for realizing topolaritons is provided by monolayers of transition metal dichalcogenides (TMDs). These atomically thin two-dimensional materials with graphenelike (honeycomb) lattice structure have attracted a lot of interest in recent years owing to their coupled spin and valley degrees of freedom, as well as their large direct band gap (1–2 eV) and interband mixing (see, e.g., Ref. [39]). In the presence of an external magnetic field that lifts their valley degeneracy [40–42], their electronic properties can be described by an effective two-band Hamiltonian of the form Eq. (5) with gap and interband-mixing parameters M and A as large as 0.5–1 eV and 3.5–4.5 eV Å, respectively [39,43,44]. Exciton-polaritons in the strong-coupling regime have also been achieved, with exciton binding energies close to 1 eV and a Bohr radius of the order of 1 nm [45]. With such parameters, the size of the exciton-photon coupling for a monolayer TMD would be of the order of 20 meV, leading to similar topological gaps as for the CdTe multi-quantum-well setups discussed above ($\Delta = 0.3$ meV for periodic exciton potentials of depth 1 meV). Such a gap would require a magnetic field of about 1.5 T to lift the valley degeneracy [40–42], corresponding to a regime where the magnetic length is much larger than the exciton Bohr radius, as desired. We remark that TMDs would also provide a promising platform to realize topolaritons with winding number $|m| = 2$ using circularly polarized light, as discussed in the Supplemental Material [26]. In that case, the circular polarization of light automatically selects one of the two valleys, thus obviating the need for a magnetic field [46–48].

For the photonic part, as mentioned above, the most practical way towards topolaritons is a two-dimensional cavity with a tailored TM gap (e.g., by using a photonic crystal). This avoids the difficult large in-plane momentum regime and leads to a true topological protection of the edge mode. Note that polaritons have been observed in photonic crystals [49], which were also recently used to reach very strong exciton-photon couplings [37].

IV. PROBING TOPOLARITONS

The nontrivial topology of topolaritons manifests itself through the existence of chiral edge modes in the excitation spectrum. Probing these modes requires both a means to excite them and the ability to observe them. Because of their mixed exciton-photon nature, chiral edge polaritons can be excited either electronically or optically. Possible electronic injection processes include exciton tunneling [50] or resonant electron tunneling [51]. More commonly, polaritons can be created by addressing their photonic component using a pump laser. Either way, the spectral resolution of the injection process should ideally be smaller than the topological gap in order to single out the chiral edge modes of interest from the rest of the spectrum. A lower spectral resolution can be compensated by better spatial focusing at the edge where the bulk modes have less weight using, e.g., laser spot sizes $<a$.

Once excited, topological polaritonic edge modes propagate chirally, which results in clear differences when observing them upstream and downstream along the edge. Although these chiral edge modes are protected from backscattering, exciton and photon losses translate as a decay of their wave function over time. Such dissipation is both harmful and useful: On one hand, the finite decay rate eventually spoils the stability of the edge mode and should not exceed the size of the topological gap for the edge modes to be well defined; on the other hand, photon losses

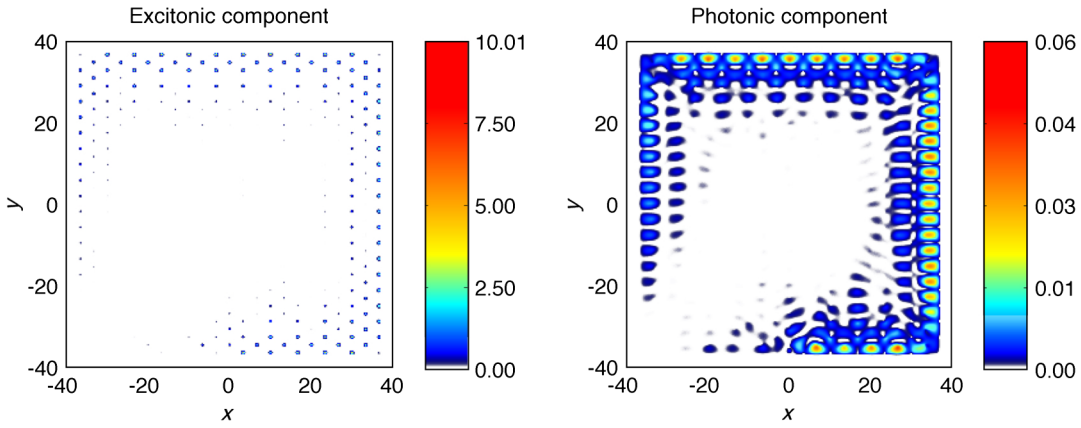

FIG. 7. Topolariton edge modes. The figure depicts the typical intensities of the exciton and photon fields obtained when pumping a finite square system optically at the center of its lower edge, shown here at time $t = 4 \times 10^3$ after switching on the laser for a triangular-lattice exciton potential of strength $V_X = -0.05$ and lattice constant $a = 3.86$. Units are defined here by setting ω_0^X and the speed of light to unity (other relevant parameters are $m_X = 1 \times 10^3$, $g_q = 0.1$, the pumping frequency $\omega_p = 0.856$, and a polariton decay rate $\gamma = 5 \times 10^{-4}$). A counterclockwise chiral edge mode is clearly visible, with an exciton component strongly peaked at the minima of the periodic potential. Exciton and photon fields both travel together as a unique polaritonic chiral edge mode.

provide a way to probe the existence of edge modes. For example, photons confined in a waveguide cannot escape when propagating along a smooth edge. Sharp turns (such as corners) would allow them to couple to the outside continuum of modes, which could be used to locally detect or inject topological polaritonic edge modes.

To incorporate pumping and loss effects and to complement the lattice-model results of Fig. 6, we simulate what we envision as a typical probe experiment using a driven-dissipative Gross-Pitaevskii equation based on the continuum model of our proposal (see Supplemental Material [26]). We consider a scenario where a continuous-wave pump laser with a frequency ω_p set within the topological gap is switched on at some initial time $t = 0$ and focused onto a spot of diameter $\approx a$ at the edge. Figure 7 shows the time-evolved exciton and photon fields obtained in that case. The photonic part of the edge modes can in principle be easily retrieved by detecting the light leaking out of the system. For example, the photon component shown in Fig. 7 would be observed in a system with uniform losses, by detecting photons escaping from the cavity in the z direction. We remark that exciton-exciton interactions are expected to be present in typical experimental realizations (see, e.g., Ref. [27]). Our numerical studies indicate that the edge modes remain stable in the presence of weak interactions (i.e., for interactions leading to a blueshift smaller than the topological gap), as expected from their chiral nature (see Supplemental Material and Video [26]).

V. CONCLUSIONS

In this paper, we show that topological polaritons ("topolaritons") are created by combining ordinary photons and excitons. The key ingredients of our scheme are a winding exciton-photon coupling and a suitable exciton potential to open a topological gap. Promising candidates for the realization of the winding coupling are two-dimensional TE-polarized photonic modes coupled to semiconductor quantum wells or monolayer transition metal dichalcogenides under a finite magnetic field. Although combining all necessary ingredients may be experimentally challenging, we emphasize that all underlying requirements have already been achieved. Realizing topolaritons thus seems within experimental reach. In light of the importance of a Brillouin zone for the opening of the gap, it would be interesting to study whether our proposal can be extended to systems known to exhibit strong polariton potentials, such as lattices of coupled micropillars [52].

Topolaritons manifest themselves through chiral edge modes which are, by definition, protected against backscattering. The directionality of these one-way channels can in principle easily be reversed, either by flipping the direction of the magnetic field or by addressing their time-reversed partners appearing at different energies. This makes for a versatile platform for the directed propagation of excitons and photons, with the possibility of converting between the two.

An important feature of topolaritons is their strong excitonic component, which allows for interactions to come into play. Interaction effects are notoriously hard to achieve in purely photonic topological systems [33]. Here, they could provide, in particular, an alternative and more flexible way to realize the periodic exciton potential required in our proposal. Indeed, one may envision the creation of an effective potential by injecting a different exciton species with a periodic density profile [53]. Interactions may also lead to novel avenues towards the observation of other intriguing topological phenomena such as nonequilibrium fractional quantum-Hall effects [8,54,55].

More broadly, our route to obtaining topological polaritons reveals a generic approach for achieving nontrivial topological states by mixing trivial bosonic components. We expect extensions of this idea to other physical systems to lead to the realization of yet more surprising bosonic topological phenomena.

ACKNOWLEDGMENTS

We are grateful to Bernd Rosenow, Alexander Janot, and Andrei Faraon for valuable discussions. This work was funded by the Institute for Quantum Information and Matter, a NSF Physics Frontiers Center with support of the Gordon and Betty Moore Foundation through Grant No. GBMF1250, NSF through No. DMR-1410435, the David and Lucile Packard Foundation, the Bi-National Science Foundation and I-Core: the Israeli Excellence Center "Circle of Light," and Darpa under funding for FENA. Support from the Swiss National Science Foundation (SNSF) is also gratefully acknowledged.

APPENDIX A: DERIVATION OF THE WINDING EXCITON-PHOTON COUPLING

Applying the minimal coupling substitution $\mathbf{k} \to \mathbf{k} + e\hat{\mathbf{A}}$ to the second-quantized representation of the quantum-well Hamiltonian Eq. (5) leads to an electron-photon coupling of the form

$$\hat{H}_{\text{el-ph}} = -iA\sum_{\mathbf{q},\mathbf{k}} F_{\mathbf{q}} \frac{1}{q}[q_x - iq_y]\hat{c}^{\dagger}_{c\mathbf{k}+\mathbf{q}}\hat{c}_{v\mathbf{k}}\hat{a}_{\mathbf{q}} + \text{H.c.}, \quad \text{(A1)}$$

where we focus on the region around the exciton-photon resonance. Note that we replace the electron operators corresponding to the original angular-momentum basis [see Eq. (5) by conduction- and valence-band operators. Both bases are related by a band-mixing-induced rotation of the order of Ak/M and are equivalent under the assumption that A/M is small as compared to the Bohr radius $a_0 \sim 1/k$ of the excitons. We verify numerically that the winding remains unchanged for larger $A/(Ma_0) \sim 1$ (for excitons with s-wave character). In that case, however, the amplitude of the exciton-photon coupling becomes suppressed.

To express the electron-photon coupling in terms of excitons, we invert Eq. (6) as $c^{\dagger}_{c,\mathbf{k}+\mathbf{q}/2}c_{v,\mathbf{k}-\mathbf{q}/2} = \sum_n \phi^*_n(\mathbf{k})\hat{b}^{(n)\dagger}_{\mathbf{q}}$. Focusing on energies close to the lowest-lying exciton allows for dropping terms including higher exciton modes with $n > 1$. With the two-dimensional Fourier transform of the s-wave wave function $\phi_1(k) = 2\sqrt{2\pi}a_0[1 + (ka_0)^2]^{-3/2}$, we then obtain Eq. (8) of the main text.

Note that the apparent nonanalyticity of Eq. (8) at $q = 0$ is an artifact of focusing only on the TE mode. For a small in-plane momentum component, the TM-polarized modes can no longer be neglected. In fact, the TE and TM polarization modes have equally large in-plane electric fields if the momentum points predominately in the z direction. In this regime, the basis of right- and left-handed circular polarizations is more suitable, and one finds a large constant coupling to the, say, right-handed mode, while the left-handed mode has a coupling with a double winding vanishing as q^2. (See Supplemental Material for more details [26]. The momentum-dependent switch from linear to circular polarization was also discussed in Ref. [56]). One can focus on the exciton-TE-photon coupling when the exciton is resonant with the TE mode at frequencies where the TM mode is gapped.

APPENDIX B: TOPOLOGICAL GAP OPENING FOR A TWO-DIMENSIONAL BRILLOUIN ZONE

Assuming a square Brillouin zone, a gap of size V_X opens at the point $X = (\pi/a, 0)$, similarly to that in Fig. 5. The main deviation from the one-dimensional case is the finite energy difference between the polaritons at the points X and $M = (\pi/a, \pi/a)$. For a global gap, V_X should be larger than $\omega^{P-}_M - \omega^{P-}_X$. Note that V_X also increases the repulsion between exciton bands backfolded into the first Brillouin zone from regions of the spectrum far away from resonance. These backfolded excitons are in an energy range $\omega^X_0 \pm 2V_X$. There is, therefore, a trade-off between the large exciton-photon coupling required to separate the lowest polariton band from the backfolded excitons [large $g^2_M/(\omega^C_M - \omega^X_0)$ as compared to V_X] and the large V_X required to open a global gap. To satisfy these requirements in the best possible way, the Brillouin zone should be as circular as possible (e.g., hexagonal) to minimize the energy difference between the points located at its boundary. For an optimal choice of a, V_X, and Brillouin-zone geometry, we expect the size of the gap to be determined by the smallest of the two values V_X and $g^2_M/(\omega^C_M - \omega^X_0)$.

[1] F. D. M. Haldane and S. Raghu, *Possible Realization of Directional Optical Waveguides in Photonic Crystals with Broken Time-Reversal Symmetry*, Phys. Rev. Lett. **100**, 013904 (2008).

[2] S. Raghu and F. D. M. Haldane, *Analogs of Quantum-Hall-Effect Edge States in Photonic Crystals*, Phys. Rev. A **78**, 033834 (2008).

[3] Z. Wang, Y. Chong, J. D. Joannopoulos, and M. Soljacic, *Observation of Unidirectional Backscattering-Immune Topological Electromagnetic States*, Nature (London) **461**, 772 (2009).

[4] Y. Poo, R.-x. Wu, Z. Lin, Y. Yang, and C. T. Chan, *Experimental Realization of Self-Guiding Unidirectional Electromagnetic Edge States*, Phys. Rev. Lett. **106**, 093903 (2011).

[5] L. D. Landau and E. M. Lifshitz, in *Electrodynamics of Continuous Media*, A Course of Theoretical Physics, Vol. 8 (Pergamon Press, New York, 1960).

[6] K. Fang, Z. Yu, and S. Fan, *Realizing Effective Magnetic Field for Photons by Controlling the Phase of Dynamic Modulation*, Nat. Photonics **6**, 782 (2012).

[7] M. C. Rechtsman, J. M. Zeuner, Y. Plotnik, Y. Lumer, D. Podolsky, F. Dreisow, S. Nolte, M. Segev, and A. Szameit, *Photonic Floquet Topological Insulators*, Nature (London) **496**, 196 (2013).

[8] J. Cho, D. G. Angelakis, and S. Bose, *Fractional Quantum Hall State in Coupled Cavities*, Phys. Rev. Lett. **101**, 246809 (2008).

[9] J. Koch, A. A. Houck, K. L. Hur, and S. M. Girvin, *Time-Reversal-Symmetry Breaking in Circuit-QED-Based Photon Lattices*, Phys. Rev. A **82**, 043811 (2010).

[10] R. O. Umucalilar and I. Carusotto, *Artificial Gauge Field for Photons in Coupled Cavity Arrays*, Phys. Rev. A **84**, 043804 (2011).

[11] M. Hafezi, E. A. Demler, M. D. Lukin, and J. M. Taylor, *Robust Optical Delay Lines with Topological Protection*, Nat. Phys. **7**, 907 (2011).

[12] M. Hafezi, S. Mittal, J. Fan, A. Migdall, and J. M. Taylor, *Imaging Topological Edge States in Silicon Photonics*, Nat. Photonics **7**, 1001 (2013).

[13] G. Q. Liang and Y. D. Chong, *Optical Resonator Analog of a Two-Dimensional Topological Insulator*, Phys. Rev. Lett. **110**, 203904 (2013).

[14] N. Jia, A. Sommer, D. Schuster, and J. Simon, *Time Reversal Invariant Topologically Insulating Circuits*, arXiv:1309.0878.

[15] V. Yannopapas, *Topological Photonic Bands in Two-Dimensional Networks of Metamaterial Elements*, New J. Phys. **14**, 113017 (2012).

[16] A. B. Khanikaev, S. Hossein Mousavi, W.-K. Tse, M. Kargarian, A. H. MacDonald, and G. Shvets, *Photonic Topological Insulators*, Nat. Mater. **12**, 233 (2013).

[17] W.-J. Chen, S.-J. Jiang, X.-D. Chen, J.-W. Dong, and C. T. Chan, *Experimental Realization of Photonic Topological Insulator in a Uniaxial Metacrystal Waveguide*, Nat. Commun. **5**, 5782 (2014).

[18] N. H. Lindner, G. Refael, and V. Galitski, *Floquet Topological Insulator in Semiconductor Quantum Wells*, Nat. Phys. **7**, 490 (2011).

[19] A. Figotin and I. Vitebskiy, *Electromagnetic Unidirectionality in Magnetic Photonic Crystals*, Phys. Rev. B **67**, 165210 (2003).

[20] Z. Yu, G. Veronis, Z. Wang, and S. Fan, *One-Way Electromagnetic Waveguide Formed at the Interface*

between a Plasmonic Metal under a Static Magnetic Field and a Photonic Crystal, Phys. Rev. Lett. **100**, 023902 (2008).

[21] Z. Wang, Y. D. Chong, J. D. Joannopoulos, and M. Soljacic, *Reflection-Free One-Way Edge Modes in a Gyromagnetic Photonic Crystal*, Phys. Rev. Lett. **100**, 013905 (2008).

[22] H. Takeda and S. John, *Compact Optical One-Way Waveguide Isolators for Photonic-Band-Gap Microchips*, Phys. Rev. A **78**, 023804 (2008).

[23] Y. Hadad and B. Z. Steinberg, *Magnetized Spiral Chains of Plasmonic Ellipsoids for One-Way Optical Waveguides*, Phys. Rev. Lett. **105**, 233904 (2010).

[24] In fact, the resulting edge modes in our case are predominantly of excitonic character, which stresses that the semiconductor degrees of freedom are more important for the nontrivial topology than simply providing an effective magneto-optical coupling.

[25] R. Winkler, *Spin-Orbit Coupling Effects in Two-Dimensional Electron and Hole Systems* (Springer, New York, 2003).

[26] See Supplemental Material at http://link.aps.org/supplemental/10.1103/PhysRevX.5.031001 for a study of the full Hamiltonian including two exciton and two photon modes as well as details regarding the Gross-Pitaevskii equation.

[27] H. Deng, H. Haug, and Y. Yamamoto, *Exciton-Polariton Bose-Einstein Condensation*, Rev. Mod. Phys. **82**, 1489 (2010).

[28] J. D. Joannopoulos, S. G. Johnson, J. N. Winn, and R. D. Meade, *Photonic Crystals: Molding the Flow of Light* (Princeton University Press, Princeton, NJ, 2011).

[29] J. Yuen-Zhou, S. S. Saikin, N. Y. Yao, and A. Aspuru-Guzik, *Topologically Protected Excitons in Porphyrin Thin Films*, Nat. Mater. **13**, 1026 (2014).

[30] D. I. Pikulin and T. Hyart, *Interplay of Exciton Condensation and the Quantum Spin Hall Effect in InAs/GaSb Bilayers*, Phys. Rev. Lett. **112**, 176403 (2014).

[31] J. C. Budich, B. Trauzettel, and P. Michetti, *Time Reversal Symmetric Topological Exciton Condensate in Bilayer HgTe Quantum Wells*, Phys. Rev. Lett. **112**, 146405 (2014).

[32] E. Yablonovitch, *Inhibited Spontaneous Emission in Solid-State Physics and Electronics*, Phys. Rev. Lett. **58**, 2059 (1987).

[33] I. Carusotto and C. Ciuti, *Quantum Fluids of Light*, Rev. Mod. Phys. **85**, 299 (2013).

[34] M. M. de Lima, M. van der Poel, P. V. Santos, and J. M. Hvam, *Phonon-Induced Polariton Superlattices*, Phys. Rev. Lett. **97**, 045501 (2006).

[35] E. A. Cerda-Méndez, D. Sarkar, D. N. Krizhanovskii, S. S. Gavrilov, K. Biermann, M. S. Skolnick, and P. V. Santos, *Exciton-Polariton Gap Solitons in Two-Dimensional Lattices*, Phys. Rev. Lett. **111**, 146401 (2013).

[36] In particular, we find well-defined topological gaps in the regime of a periodic-potential-induced TM gap as discussed in the Supplemental Material [26].

[37] J.-H. Jiang and S. John, *Photonic Crystal Architecture for Room-Temperature Equilibrium Bose-Einstein Condensation of Exciton Polaritons*, Phys. Rev. X **4**, 031025 (2014).

[38] A. A. Sirenko, T. Ruf, M. Cardona, D. R. Yakovlev, W. Ossau, A. Waag, and G. Landwehr, *Electron and Hole g Factors Measured by Spin-Flip Raman Scattering in* $CdTe/Cd_{1-x}Mg_xTe$ *Single Quantum Wells*, Phys. Rev. B **56**, 2114 (1997).

[39] D. Xiao, G.-B. Liu, W. Feng, X. Xu, and W. Yao, *Coupled Spin and Valley Physics in Monolayers of* MoS_2 *and Other Group-VI Dichalcogenides*, Phys. Rev. Lett. **108**, 196802 (2012).

[40] D. MacNeill, C. Heikes, K. F. Mak, Z. Anderson, A. Kormányos, V. Zólyomi, J. Park, and D. C. Ralph, *Breaking of Valley Degeneracy by Magnetic Field in Monolayer* $MoSe_2$, Phys. Rev. Lett. **114**, 037401 (2015).

[41] A. Srivastava, M. Sidler, A. V. Allain, D. S. Lembke, A. Kis, and A. Imamoğlu, *Valley Zeeman Effect in Elementary Optical Excitations of Monolayer* WSe_2, Nat. Phys. **11**, 141 (2015).

[42] G. Aivazian, Z. Gong, A. M. Jones, R.-L. Chu, J. Yan, D. G. Mandrus, C. Zhang, D. Cobden, W. Yao, and X. Xu, *Magnetic Control of Valley Pseudospin in Monolayer* WSe_2, Nat. Phys. **11**, 148 (2015).

[43] T. Cai, S. A. Yang, X. Li, F. Zhang, J. Shi, W. Yao, and Q. Niu, *Magnetic Control of the Valley Degree of Freedom of Massive Dirac Fermions with Application to Transition Metal Dichalcogenides*, Phys. Rev. B **88**, 115140 (2013).

[44] F. Rose, M. O. Goerbig, and F. Piéchon, *Spin- and Valley-Dependent Magneto-optical Properties of* MoS_2, Phys. Rev. B **88**, 125438 (2013).

[45] X. Liu, T. Galfsky, Z. Sun, F. Xia, E.-c. Lin, Y.-H. Lee, S. Kéna-Cohen, and V. M. Menon, *Strong Light-Matter Coupling in Two-Dimensional Atomic Crystals*, Nat. Photonics **9**, 30 (2015).

[46] T. Cao, G. Wang, W. Han, H. Ye, C. Zhu, J. Shi, Q. Niu, P. Tan, E. Wang, B. Liu, and J. Feng, *Valley-Selective Circular Dichroism of Monolayer Molybdenum Disulphide*, Nat. Commun. **3**, 887 (2012).

[47] H. Zeng, J. Dai, W. Yao, D. Xiao, and X. Cui, *Valley Polarization in* MoS_2 *Monolayers by Optical Pumping*, Nat. Nanotechnol. **7**, 490 (2012).

[48] K. F. Mak, K. He, J. Shan, and T. F. Heinz, *Control of Valley Polarization in Monolayer* MoS_2 *by Optical Helicity*, Nat. Nanotechnol. **7**, 494 (2012).

[49] D. Bajoni, D. Gerace, M. Galli, J. Bloch, R. Braive, I. Sagnes, A. Miard, A. Lemaitre, M. Patrini, and L. C. Andreani, *Exciton Polaritons in Two-Dimensional Photonic Crystals*, Phys. Rev. B **80**, 201308 (2009).

[50] I. Lawrence, S. Haacke, H. Mariette, W. W. Rühle, H. Ulmer-Tuffigo, J. Cibert, and G. Feuillet, *Exciton Tunneling Revealed by Magnetically Tuned Interwell Coupling in Semiconductor Double Quantum Wells*, Phys. Rev. Lett. **73**, 2131 (1994).

[51] H. Cao, G. Klimovitch, G. Björk, and Y. Yamamoto, *Direct Creation of Quantum Well Excitons by Electron Resonant Tunneling*, Phys. Rev. Lett. **75**, 1146 (1995).

[52] T. Jacqmin, I. Carusotto, I. Sagnes, M. Abbarchi, D. D. Solnyshkov, G. Malpuech, E. Galopin, A. Lemaître, J. Bloch, and A. Amo, *Direct Observation of Dirac Cones and a Flatband in a Honeycomb Lattice for Polaritons*, Phys. Rev. Lett. **112**, 116402 (2014).

[53] A. Amo, S. Pigeon, C. Adrados, R. Houdré, E. Giacobino, C. Ciuti, and A. Bramati, *Light Engineering of the Polariton Landscape in Semiconductor Microcavities*, Phys. Rev. B **82**, 081301 (2010).

[54] R. O. Umucalilar and I. Carusotto, *Fractional Quantum Hall States of Photons in an Array of Dissipative Coupled Cavities*, Phys. Rev. Lett. **108**, 206809 (2012).

[55] M. Hafezi, M. D. Lukin, and J. M. Taylor, *Non-Equilibrium Fractional Quantum Hall State of Light*, New J. Phys. **15**, 063001 (2013).

[56] D. D. Solnyshkov, M. M. Glazov, I. A. Shelykh, A. V. Kavokin, E. L. Ivchenko, and G. Malpuech, *Magnetic Field Effect on Polarization and Dispersion of Exciton-Polaritons in Planar Microcavities*, Phys. Rev. B **78**, 165323 (2008).